Experimental demonstration of dielectric-loaded plasmonic waveguide disk resonators at telecom wavelengths

Sukanya Randhawa,[1] Alexey V. Krasavin,[2] Tobias Holmgaard,[3] Jan Renger,[1] Sergey I. Bozhevolnyi,[4] Anatoly V. Zayats,[2] and Romain Quidant[1,5,a)]
[1]*ICFO-Institut de Ciencies Fotoniques, Mediterranean Technology Park, 08860 Castelldefels (Barcelona), Spain*
[2]*Nano-optics and Near-field Spectroscopy Group, Department of Physics, King's College London, Strand, London WC2R 2LS, United Kingdom*
[3]*Department of Physics and Nanotechnology, Aalborg University, Skjernvej 4A, DK-9220 Aalborg Øst, Denmark*
[4]*Insitute of Technology and Innovation, University of Southern Denmark, Niels Bohrs Allé 1, DK-5230 Odense M, Denmark*
[5]*Institució Catalana de Recerca i Estudis Avançats (ICREA), 08010 Barcelona, Spain*

(Received 9 December 2010; accepted 17 March 2011; published online 18 April 2011)

Dielectric-loaded plasmonic waveguide disk resonators (WDRs) operating at telecom wavelengths are fabricated and investigated. Disks resonators of various radii coupled to a straight waveguide are studied both numerically and experimentally. For each disk radius, the gap between the disk and the waveguide is varied from 0 to 300 nm. Performance of the fabricated WDRs is characterized in the wavelength range of 1500–1620 nm using near-field optical microscopy. Wavelength selectivity and efficiency of the WDRs are evaluated and are in good agreement with numerical results. © *2011 American Institute of Physics*. [doi:10.1063/1.3574606]

The miniaturization of conventional photonic circuits is hindered by the diffraction limit, and the field of plasmonics has enabled an improved synergy between photonics and electronics. Surface plasmons polaritons (SPPs) are evanescent waves bounded to a metallic–dielectric interface, and therefore are promising candidates for highly integrated optics.[1] In recent years, many research groups have demonstrated control of SPP waves in two dimensions by designing structural elements that are either metallic or dielectric.[2] Recently, it has been shown that Bragg mirrors consisting of gratings of dielectric ridges deposited on a metallic surface are very efficient tools to perform this task for SPPs.[3]

Dielectric-loaded SPP waveguides (DLSPPWs) produced by a dielectric stripe (typically 500×500 nm^2 for telecom wavelengths) placed on a metal surface exhibit strong confinement and feature relatively low bend and propagation losses.[4–7] DLSPPW components such as waveguide ring resonators (WRRs) and in-line Bragg gratings can be used for wavelength selection and moreover for active control of SPP waves,[4,5] which is important for designing photonics circuits.[7] Although waveguide disk resonators (WDRs) have similar geometries to WRRs, recent theoretical studies have shown that the WDR design offers several advantages in terms of smaller radiation losses (or higher quality factors).[8] This is due to the fact that in microdisk resonators the absence of an inner cylindrical boundary permits the supported mode to reside closer to the resonator center with weaker penetration of field components in the surrounding air, which leads to smaller radiation losses.[8] WDRs are also easier to fabricate due to less rigid requirements on fabrication tolerances and are more apt candidates for tuning purposes.

In this letter, the fabrication and investigation of dielectric-loaded plasmonic WDRs operating at telecom wavelengths are presented. Based on the experimental data, the performance of WDRs is examined with respect to several key parameters, such as the disk radius and separation gap. Experimental data are compared to rigorous three-dimensional (3D) numerical simulations.

Samples containing WDR structures were fabricated using the following procedure. A 50 nm thick Au film was deposited on a glass substrate via thermal evaporation. Then, a 560 nm thick polymer poly(methyl methacrylate) (PMMA) layer was spin-coated onto the Au film. Finally, plasmonic waveguides and disk resonators were fabricated by directly patterning the PMMA film with a 30 keV electron beam and further chemical development. Low resolution effects previously observed in small separation regions between straight waveguides and disk resonators were overcome by using advanced proximity correction in the design. Scanning electron microscopy was used to confirm the waveguide width of ~500 nm and thus ensure single-mode DLSPPW operation. In order to study the WDRs performance based on important design parameters, structures with different disk radii and various gaps sizes were fabricated [Fig. 1(a)]. The length of the funnel region L1 was chosen to be 25 μm, whereas the overall length of the waveguide L2 and the position of the disk L3 were 70 μm and 50 μm, respectively.

A scanning near-field optical microscope (SNOM), having an uncoated fiber tip, was used for characterization of the SPP transmission through the WDRs.[9] To facilitate efficient excitation of the DLSPPW mode, all waveguides were connected to taper structures. The mode was excited inside the taper by matching the excitation angle in the Kretschmann configuration and then was funneled into the waveguide. The excitation wavelength was in the 1500–1620 nm range.

The first set of structures investigated were WDRs with a radius of 4 μm and the separation gap varying from the

a)Author to whom correspondence should be addressed. Electronic mail: romain.quidant@icfo.es.

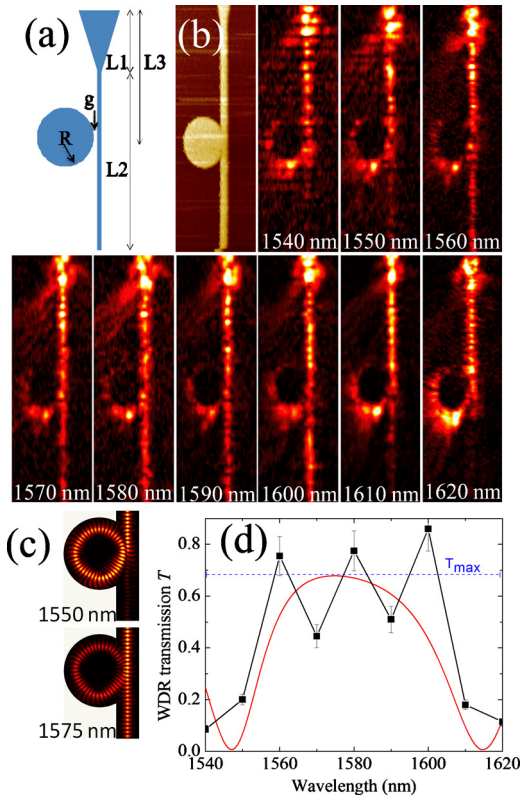

FIG. 1. (Color online) (a) Schematic of the WDR: the dielectric disk resonator made of PMMA on top of a planar Au film. (b) Topography and near-field intensity measured with a SNOM for different wavelengths in 1540–1620 nm range ($g=100$ nm, $R=4$ μm). (c) Numerically calculated field maps $|Re(E_z)|$ (E_z is the main component of the electric field perpendicular to the metal surface) for the same parameters as in (b), for resonant case (1550 nm) and a non-resonant case (1575 nm). (d) WDR transmission measured at the output waveguide section (squares) compared with the numerical modeling (smooth line) for the WDR parameters in (b).

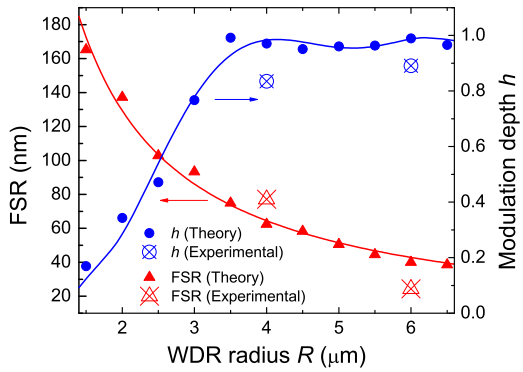

FIG. 2. (Color online) Evolution of the FSR (triangles) and modulation depth h (circles) with the disk radius at a constant gap $g=100$ nm. The crosses represent the experimental data, solid lines represent numerical results. No fitting parameters were used for numerical modeling.

contact case ($g=0$ nm) to values of 100, 200, and 300 nm. Good coupling to the disk was observed for $g=100$ nm, as shown in Fig. 1(b) by the optical near-field intensity images which were acquired at various wavelengths. Whenever the DLSPPW mode was coupled to the disk, a stop-band filter behavior was observed. A plot of the WDR transmission taken at the output waveguide section, normalized to the input, demonstrates a strong decrease in the output signal at the resonant wavelengths [Fig. 1(d)], which occurs at $\lambda=1620$ nm and 1540 nm. The minima correspond to the case when the whispering gallery disk mode propagating along the disk edge is in resonance and the waveguide mode is efficiently coupled to it. In the first approximation this happens when the optical path of the disk mode is equal to an integer number of the mode wavelengths [Fig. 1(c)]. At the same time this corresponds to the destructive interference of the waveguide mode passed through the coupling region and the component of the disk mode coupled back into the waveguide. Please note that the jumps in the experimental transmission between the two dips are most likely caused by small damages to the waveguide during scanning.

One of the main characteristics of WDR performance is the transmission period between two neighboring minima, also called the bandwidth or the free spectral range (FSR).[10] From a simple WDR transmission model described above it follows that the transmission period is mainly defined by the effective refractive index of the disk mode n_{eff} and the disk radius R. A simple estimation,

$$\text{FSR} = \lambda^2/(2\pi n_{\text{eff}} R) \tag{1}$$

gives a correct idea about its value of few tens of nanometers observed in the experiment. However, due to the fact that n_{eff} as well as coupling-induced phase shift (CIFS) (Ref. 11) are actually wavelength-dependent, a more comprehensive theoretical approach is necessary. Full 3D numerical simulations based on the finite element method were employed to study the WDR transmission. The numerical prediction [Fig. 1(d), line] is in good agreement with experimental results. Here, the ring radius R, which can be different due to the limited fabrication precision, was used as a fitting parameter ($R_{\text{num}}=3.925$ μm). The transmission curve was found to be rather independent on the gap in the range of 100–200 nm, so it was kept at 100 nm as specified during fabrication. It was further studied how the FSR depends on the disk radius, while the separation gap g is kept constant at 100 nm. As one can see from Fig. 2, the numerical curve (triangles) for FSR, follows 1/R dependence, predicted by Eq. (1). The simulation curves have been validated by experimental results (data points). The transmission period (data points) decreases from 64 to 25 nm as the disk radius is changed from 4 to 6 μm, which is in general agreement with theoretical predictions. The experimental points are slightly mismatched compared to the simulation values because the disk resonator configuration is very sensitive to slight changes in geometry due to fabrication imperfections.

Another important parameter which benchmarks the disk performance is the modulation depth $h=(T_{\max}-T_{\min})/(T_{\max}+T_{\min})$. Numerical simulations performed for all the considered radii from 1.5 to 6.5 μm in incremental steps of 0.5 μm with a fixed gap $g=100$ nm, show that for smaller radii the modulation depth is rather small. This is due to the fact that the mode suffers from significant radiation losses,[8] and thus, coupled in the waveguide output does not significantly influence the interference outcome. Then, through the region of $R=2.5-3.5$ μm the modulation depth increases and at radii larger than 3.5 μm it saturates at the level close to 100%. Taking into account that the maximum transmission $T_{\max}$ [Fig. 1(d)] monotonically decreases for radii $R>4.5$ μm (from $T_{\max}=0.7$ at $R=4$ μm to $T_{\max}=0.5$ at $R=6.5$ μm), we can conclude that the WDR disk radius around $R=4$ μm is the optimal in terms of modulation depth

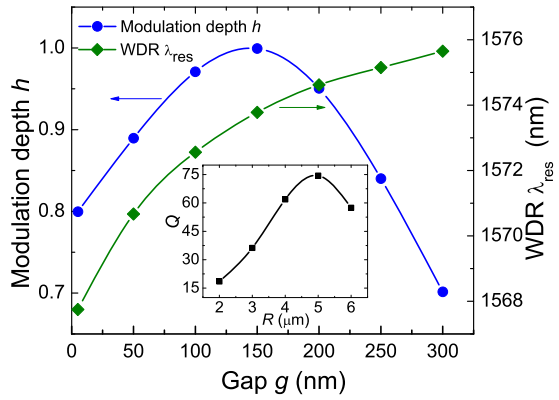

FIG. 3. (Color online) Numerical results: dependence of the modulation depth h (circles) and WDR resonant wavelength λ_{res} (diamonds) and on the separation gap at a constant disk radius $R=4\ \mu$m. The inset shows the dependence of the quality factor Q on the disk radius.

– maximum transmission trade-off. If we consider the quality factor $Q=\lambda_{res}/\Delta\lambda$ (λ_{res} is the resonant wavelength, $\Delta\lambda$ is its full width half maximum) to be the value which benchmarks the WDR performance, then the optimal radius at $R=5\ \mu$m with $Q\sim 75$ (see inset to Fig. 3) is not much different from the optimum radius in terms of modulation depth. From the experimental results we estimated $Q\sim 55$ for $R=4\ \mu$m and $Q\sim 105$ for $R=6\ \mu$m.

The separation gap between the waveguide and the resonant disk plays an important role in determining the coupling strength of the resonant disk mode. For each disk radius there is an optimal gap corresponding to the largest modulation depth. This has been confirmed by the experimental images for $R=4\ \mu$m (not shown here) and different gap sizes ranging from $g=0$ nm (the contact case) to $g=300$ nm. Figure 3 shows the simulation response of the modulation depth h, when the gap is varied (circles). We observed a drop in the modulation depth when the gap is too large or when it is zero. For modulation depth an optimal evolution is seen with respect to the increasing gap size between the waveguide and the disk. It is largely dependent on the coupling strength, SPP propagation loss and the bend losses which are associated with the radius of the disk do not play an important role in this study, as the radius of the disk is kept constant. Naturally, there is a slight change in the resonant wavelength λ_{res} when the gap changes (Fig. 3, diamonds), which is connected with the CIFSs.[11]

In conclusion, we have realized efficient and compact wavelength selective DLSPP disk resonators which operate at telecom wavelengths. With the aid of experimental data based on SNOM characterization and further numerical modeling, we have analyzed the role of various important parameters such as the disk radius and gap separation, and how they can be used to optimize the device performance in terms of the modulation depth and wavelength selectivity. The disk resonator design is not just superior to its ring counterpart because of easier fabrication and smaller radiation losses but also provides slightly better performance in wavelength selection for integrated photonic circuitry.

This work was supported by EC FP6 STREP PLASMOCOM. T.H. and S.I.B. also acknowledge the support of the FTP Project No. 09-072949 ANAP. A.K. and A.Z. acknowledge support from EPSRC (UK).

[1]W. L. Barnes, A. Dereux, and T. W. Ebbesen, Nature (London) **424**, 824 (2003).
[2]*Plasmonic Nanowaveguides and Circuits*, edited by S. I. Bozhevolnyi (Pan Stanford, Singapore, 2008).
[3]S. Randhawa, M. U. González, J. Renger, S. Enoch, and R. Quidant, Opt. Express **18**, 14496 (2010).
[4]J. Gosciniak, S. I. Bozhevolnyi, T. B. Andersen, V. S. Volkov, J. Kjelstrup-Hansen, L. Markey, and A. Dereux, Opt. Express **18**, 1207 (2010).
[5]A. V. Krasavin and A. V. Zayats, Opt. Commun. **283**, 1581 (2010).
[6]A. V. Krasavin and A. V. Zayats, Opt. Express **18**, 11791 (2010).
[7]T. Holmgaard, S. I. Bozhevolnyi, L. Markey, and A. Dereux, Appl. Phys. Lett. **94**, 051111 (2009).
[8]O. Tsilipakos and E. E. Kriezis, Opt. Commun. **283**, 3095 (2010).
[9]T. Holmgaard, S. I. Bozhevolnyi, L. Markey, A. Dereux, A. V. Krasavin, P. Bolger, and A. V. Zayats, Phys. Rev. B **78**, 165431 (2008).
[10]K. Oda, N. Takato, and H. Toba, J. Lightwave Technol. **9**, 728 (1991).
[11]M. A. Popović, C. Manolatou, and M. R. Watts, Opt. Express **14**, 1208 (2006).